Journal of Molecular Science

Journal of Molecular Science
Volume 36 Issue 2, Year of Publication 2026, Page 495-504
DoI-10.004687/1000-9035.2026.059

Journal of Molecular Science
www.jmolecularsci.com ISSN:1000-9035

Optimized Acrylamide-Grafted *Eucalyptus obliqua* Gum as a Novel Carrier for Sulfasalazine: Synthesis, Characterization, and In Vitro Drug Release

Naimish Nanda[1*], Ravindra B. Laware[2]
[1]College of Pharmaceutical Sciences, Bhagwant University, Ajmer, Rajasthan, India
[2]College of Pharmaceutical Sciences, Faculty of Pharmacy, Pravara Institute of Medical Sciences (Deemed to Be University), Loni, Maharashtra, India.

Article Information
Received: 21-05-2026
Revised: 04-06-2026
Accepted: 20-06-2026
Published: 05-07-2026

Keywords
Eucalyptus obliqua gum; Acrylamide grafting; Box-Behnken design; Sulfasalazine; Matrix tablet; Sustained release; Release kinetics.

ABSTRACT
Sulfasalazine is a poorly water-soluble anti-inflammatory drug used in inflammatory bowel disease that requires a sustained-release carrier to reduce dosing frequency and improve colonic residence. In the present study, Eucalyptus obliqua gum, a plant-derived polysaccharide, was chemically modified by microwave-assisted grafting with acrylamide using ceric ammonium nitrate as initiator, and the process was optimized by a three-factor, three-level Box-Behnken design (BBD) with monomer amount, initiator amount and reaction temperature as independent variables and % yield, % grafting and % grafting efficiency as responses. Design-Expert software generated quadratic models with high R^2 (>0.94) for all three responses, and numerical optimization identified 1.4 g acrylamide and 50 mg ceric ammonium nitrate at 60°C as the optimum grafting condition. The grafted gum was characterized by FTIR, DSC, XRD and SEM, which confirmed successful grafting, an amorphous-to-partially-crystalline transition and increased surface roughness. Swelling capacity and viscosity of the grafted gum were higher than the ungrafted gum. The grafted and ungrafted gums were subsequently evaluated as matrix-forming polymers for sulfasalazine sustained-release tablets (UEO1-UEO5, GEO1-GEO5) at five drug-to-polymer ratios. Precompression and post-compression parameters of all batches complied with pharmacopoeial limits. In vitro dissolution testing showed that grafted-gum tablets sustained drug release for up to 18 h compared with 8-10 h for ungrafted-gum tablets. The formulation GEO5 (containing the highest grafted-gum ratio) exhibited the longest mean dissolution time (9.90 h) and was selected as the optimized formulation. Release from GEO5 best fitted the Korsmeyer-Peppas model (R^2 = 0.9735, n = 1.366), indicating a super case-II transport mechanism dominated by polymer erosion and swelling. GEO5 remained physically and chemically stable under accelerated conditions (40°C ± 2°C / 75% ± 5% RH) for three months, with similarity factor (f2) values above 75 at all-time points. These findings suggest that acrylamide-grafted Eucalyptus obliqua gum is a promising, low-cost, plant-based excipient for sustained-release oral delivery of sulfasalazine.

1. INTRODUCTION:

The development of site-specific DDS has become very important in modern medicine especially for treating problems in the GI tract. Colonial drug delivery is very helpful for diseases like IBDs and colorectal cancer. This is highly desirable for treating disorders of the gastrointestinal tract also effective with colonial drug delivery. Colonial drug delivery systems are being developed to treat IBDs Such systems are a cornerstone of pharmaceutics,

Journal of Molecular Science
Volume 36 Issue 2, Year of Publication 2026, Page 495-504
DoI-10.004687/1000-9035.2026.059

for treating colorectal cancer [1,2]. The amount of Sulfasalazine delivery from the intestine to the blood stream is limited which shows less side effect. Sulfasalazine is a kind of medicine that is made up of two parts: 5-aminosalicylic acid and sulphapyridine. These two parts are connected with a special kind of bond called an azo bond. The Sulfasalazine works by staying in the intestine and helping to make the 5-aminosalicylic acid work better[3]. The Inflammatory Bowel Disease can better treat with sulfasalazine. When taken it by mouth it can get absorbed too quickly in the upper part of the digestive system. This can cause some bad side effects like feeling sick getting headaches and having stomach pain[4]. So, it is really important that the medication gets released in a way that it does not get absorbed until it is, pass stomach and the upper part of intestines. This way the Inflammatory Bowel Disease medication can work properly[5]. Natural polysaccharides are really popular because they are safe, break down easily and do not harm people. Eucalyptus obliqua gum, a type of gum that not many people know about has some great qualities like being really thick and able to form strong films. Many natural gums have problems, like dissolving too quickly and not being strong enough[6,7].

Grafting monomers like acrylamide onto the natural gum backbone is a way to change its properties. When acrylamide is added to the tablet it gets some groups that help the tablet work well in different situations and make the tablet stronger[8]. The tablet is a choice for giving out drugs in a controlled way. The acrylamide addition is very important because it helps the tablet react to changes around it like how acidic its which is a big factor in how the drug is released. The natural gum is still the part of the tablet[9,10]. The acrylamide addition makes the acrylamide grafted tablet more useful for this purpose. The acrylamide grafting makes the tablet better, at releasing drugs[11]. Furthermore, the incorporation of crosslinking agents during the synthesis process can prevent premature swelling in acidic gastric environments, ensuring that the hydrogel matrix remains intact until reaching the physiological pH of the colon[12].

2. MATERIALS AND METHODS:

Sulfasalazine was obtained as a gift sample Aspire Pharmaceuticals Pvt. Ltd. Eucalyptus obliqua gum was collected and purified in-house. Acrylamide and ceric ammonium nitrate (initiator) were of analytical/laboratory reagent grade. All other chemicals and reagents used were of analytical grade.

2.1 Preformulation studies

The organoleptic properties (colour, odour, taste, physical state), melting point (capillary fusion method and differential scanning calorimetry, DSC), Fourier-transform infrared (FTIR) spectrum, qualitative and quantitative solubility (in methanol, water, 0.1 N HCl and phosphate buffer pH 6.8), UV absorption maxima (λmax), calibration curves (0.1 N HCl and phosphate buffer pH 6.8) and n-octanol/PBS (pH 6.8) partition coefficient of sulfasalazine were determined by standard pharmacopoeial and reported spectrophotometric procedures[13].

2.2 Microwave-assisted grafting of Eucalyptus obliqua gum and Box-Behnken optimization

Acrylamide was grafted onto the Eucalyptus obliqua gum backbone by a microwave-assisted, ceric ammonium nitrate-initiated free-radical graft copolymerization method. A three-factor, three-level Box-Behnken design (Design-Expert software, version 7.0, Stat-Ease Inc., USA) was employed to study the effect of acrylamide (monomer), ceric ammonium nitrate (initiator) and reaction temperature on % yield (Y1), % grafting (Y2) and % grafting efficiency (Y3). Fifteen experimental runs generated by the design were performed, and the resulting data were fitted to quadratic polynomial models; model adequacy was assessed by ANOVA (F value, p value, R^2, adjusted R^2, predicted R^2 and adequate precision). Numerical (desirability-based) optimization was used to select the process condition giving maximum yield, grafting and grafting efficiency simultaneously; the model-predicted optimum was verified experimentally[14, 15].

2.3 Characterization of grafted gum

The ungrafted and optimized grafted Eucalyptus obliqua gum were characterized by FTIR spectroscopy, DSC (thermal behaviour), powder X-ray diffraction, XRD (crystallinity) and scanning electron microscopy, SEM (surface morphology). Swelling capacity of ungrafted and grafted gum was determined gravimetrically over 4 h, and apparent viscosity was measured using a Brookfield viscometer at 32.7°C. Drug-polymer compatibility of sulfasalazine with ungrafted and grafted Eucalyptus obliqua gum was assessed by FTIR spectroscopy of physical mixtures stored for four weeks under ambient conditions[16, 17].

2.4 Preparation and evaluation of sulfasalazine matrix tablets

Sustained-release matrix tablets of sulfasalazine were prepared using ungrafted Eucalyptus obliqua gum (batches UEO1-UEO5) and grafted Eucalyptus obliqua gum (batches GEO1-GEO5) as the matrix-forming polymer at five increasing drug-to-polymer ratios (1:0.25, 1:0.375, 1:0.5, 1:0.625 and 1:0.75), with lactose as diluent. Powder blends were evaluated for angle of repose, bulk density, tapped density, Carr's index and Hausner's ratio prior to

Journal of Molecular Science
Volume 36 Issue 2, Year of Publication 2026, Page 495-504
DoI-10.004687/1000-9035.2026.059

compression. Compressed tablets were evaluated for appearance, thickness, hardness, friability, weight variation and drug content, all as per standard pharmacopoeial methods (n = 3).

2.5 In vitro drug release, kinetics and stability

In vitro drug release was carried out using a USP type-II (paddle) dissolution apparatus at 50 rpm and 37 ± 0.5°C, using 900 mL of 0.1 N HCl for the first 2 h followed by phosphate buffer pH 6.8, with sulfasalazine estimated spectrophotometrically at 270 nm. Release data of the optimized batch were fitted to zero order, first order, Higuchi and Korsmeyer-Peppas models to elucidate the mechanism of drug release. Mean dissolution time (MDT) was calculated for all batches to select the best-performing formulation, which was then subjected to accelerated stability testing (40°C ± 2°C / 75% ± 5% RH) for three months, with organoleptic properties, hardness, drug content, friability and drug release profile monitored at monthly intervals; difference (f1) and similarity (f2) factors were calculated to compare release profiles before and after storage.

3. RESULTS AND DISCUSSION:

3.1 Preformulation studies

Sulfasalazine was obtained as an odourless, slightly bitter, crystalline yellow-brown powder. The experimentally observed melting point (161.17 ± 0.76 °C; DSC range 160.14-164.78 °C) was concordant with the reference value of 160-162 °C, confirming drug purity and identity (Table 1). FTIR analysis showed the principal absorption bands of sulfasalazine at 1672.95 cm^{-1} (C=O stretching), 3299.41 cm^{-1} and 3213.81 cm^{-1} (N-H and O-H stretching) and 1259.17/1178.18 cm^{-1} (asymmetric/symmetric C-O-C stretching), consistent with reference spectra and confirming drug authenticity.

Sulfasalazine showed the highest solubility in 0.1 N HCl (236.73 ± 3.22 mg/mL) followed by water (156.77 ± 3.14 mg/mL), phosphate buffer pH 6.8 (82.09 ± 1.52 mg/mL) and methanol (24.75 ± 1.68 mg/mL). The drug obeyed Beer-Lambert's law in the 5-30 µg/mL range at λmax 270 nm in both dissolution media used (0.1 N HCl and phosphate buffer pH 6.8), validating the analytical method used for subsequent quantification. The experimental n-octanol/PBS (pH 6.8) partition coefficient (-1.4 ± 0.002) closely matched the literature value (-1.46), confirming the hydrophilic character of the drug.

Table 1. Preformulation characterization of sulfasalazine

Parameter	Reference value	Observed value
Melting point (capillary method)	160-162 °C	161.17 ± 0.76 °C
Melting point (DSC range)	25°C to 220°C	160.14-164.78 °C
λmax (UV)	270 nm	270 nm
Partition coefficient (n-octanol:PBS pH 6.8)	-1.46	-1.4 ± 0.002

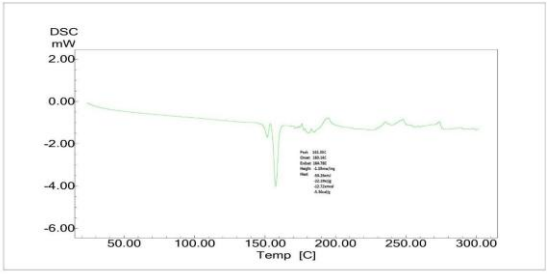

Figure 1. DSC thermograph of sulfasalazine

3.2 Box-Behnken optimization of acrylamide grafting onto Eucalyptus obliqua gum

Fifteen experimental runs of the Box-Behnken design gave % yield ranging from 22.09% to 75.89%, % grafting from 16% to 242%, and % grafting efficiency from 3.07% to 51.58% (Table 2). ANOVA of the quantitative model for % yield showed the model to be highly significant ($F = 105.66$, $p < 0.0001$) with $R^2 = 0.9948$, adjusted $R^2 = 0.9854$ and predicted $R^2 = 0.9656$, and a non-significant lack-of-fit ($p = 0.8239$), confirming good fit and predictive ability. Monomer (acrylamide) amount was the most influential factor ($p < 0.0001$), followed by initiator amount and temperature, with significant interaction and quadratic terms.

Quadratic model for % Yield (Y1): $Y1 = 52.66 - 9.01A + 5.93B + 3.85C + 5.04AB - 3.88AC + 2.94BC + 12.33A^2 - 17.08B^2 - 6.58C^2$

Similarly, quadratic models for % grafting and % grafting efficiency showed acceptable fit statistics, and both increased with increasing monomer amount up to an optimum, beyond which excessive homopolymerization reduced grafting efficiency. Numerical optimization predicted an optimum condition of 1.4 g acrylamide and 50 mg ceric ammonium nitrate at 60°C, giving predicted values of 75.13% yield, 212.47% grafting and 50.87% grafting efficiency (batch S4, Table 3). Experimental verification of the batch (73.33% yield, 186% grafting, 48.94% grafting efficiency) was in close agreement with the predicted values, confirming model validity; this batch was therefore selected as the optimized grafted Eucalyptus obliqua gum (referred to as "grafted gum" hereafter) for further studies.

Journal of Molecular Science
Volume 36 Issue 2, Year of Publication 2026, Page 495-504
DoI-10.004687/1000-9035.2026.059

Table 2. Box-Behnken design matrix and observed responses for grafting of Eucalyptus obliqua gum

Code	Acrylamide (g)	Initiator (mg)	Temp (°C)	% Yield	% Grafting	% Grafting efficiency
EOA1	2.1	50	50	50.57	168	32.31
EOA2	1.4	75	50	57.01	125.2	32.95
EOA3	2.1	50	50	52.08	176	33.85
EOA4	1.4	50	40	60.51	136	35.79
EOA5	1.4	25	50	55.17	112.4	28.58
EOA6	2.8	75	50	50.67	242	34.67
EOA7	2.8	50	60	48.48	224.8	34.06
EOA8	2.1	75	40	28.04	50	9.62
EOA9	2.1	25	60	24.00	26	5.00
EOA10	2.1	50	50	55.25	192.8	37.08
EOA11	2.1	25	40	22.10	16	3.08
EOA12	2.8	50	40	48.63	225.8	34.21
EOA13	2.1	75	60	41.72	123.2	23.69
EOA14	1.4	50	60	75.90	210	51.58
EOA15	2.8	25	50	28.66	90.6	13.73

Table 3. Checkpoint (numerical optimization) batches for grafted Eucalyptus obliqua gum. %Y = % yield, %G = % grafting, %GE = % grafting efficiency.

Checkpoint	Acrylamide (g)	Initiator (mg)	Temp (°C)	Pred. %Y	Exp. %Y		Pred. %G	Exp. %G	Pred. %GE	Exp. %GE
S1	1.4	75	50	57.79	51.79		119.87	104.6	33.68	27.52
S2	2.8	75	50	49.83	45.33		239.07	206	33.91	31.21
S3	1.4	50	40	59.66	52.46		135.92	104.6	34.99	27.52
S4 (selected)	1.4	50	60	75.13	73.33		212.47	186	50.87	48.94
S5	2.8	50	40	49.38	40.29		223.32	170	34.91	25.75

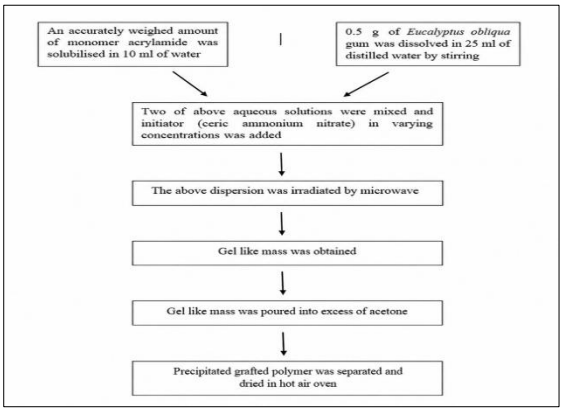

Figure 2. Schematic representation of microwave-assisted acrylamide grafting onto Eucalyptus obliqua gum

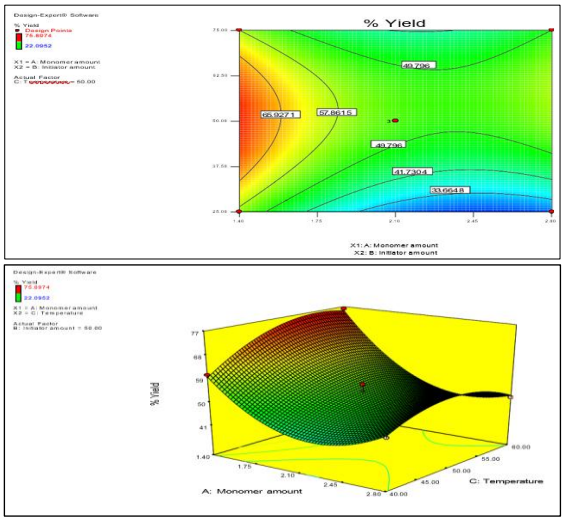

Figure 3. Contour plot and 3D response surface showing the effect of acrylamide amount and initiator amount on % yield (Y1)

3.3 Characterization of grafted gum

FTIR spectra of ungrafted Eucalyptus obliqua gum showed characteristic C-H stretching (2918.92 cm^{-1}), C=O stretching (1698.78 cm^{-1}) and =C-H bending (951.12 cm^{-1}). Acrylamide showed NH stretching at 3355.65 cm^{-1}, C=O stretching at 1647 cm^{-1} and CN stretching near 1351.92 cm^{-1}. The grafted gum spectrum showed a broadened absorption band around 2926 cm^{-1} arising from overlap of the gum O-H stretch and acrylamide N-H stretch, confirming covalent grafting (Figure 2).

XRD analysis showed the ungrafted gum to be largely amorphous, while acrylamide displayed sharp crystalline peaks; the grafted gum retained the acrylamide-characteristic peaks but with markedly reduced intensity, consistent with the formation of a graft copolymer in which acrylamide chains are incorporated into an amorphous gum matrix. SEM images showed the grafted gum surface to be rougher and more irregular than the smooth surface of the ungrafted gum, attributable to deposition/grafting of acrylamide chains onto the polysaccharide backbone (Figure 3). DSC thermograms showed an increase in glass transition/thermal event temperature for the grafted gum relative to the ungrafted gum and acrylamide individually, consistent with restricted chain mobility following grafting.

The swelling capacity of the grafted gum (716% at 240 min) was more than double that of the ungrafted gum (389.5% at 240 min), attributed to the increased number of hydrophilic polysaccharide/acrylamide chains and greater porosity of the grafted network (Table 4). Similarly, the apparent viscosity of the

Journal of Molecular Science
Volume 36 Issue 2, Year of Publication 2026, Page 495-504
DoI-10.004687/1000-9035.2026.059

grafted gum (1188.6 ± 1.4 cps) was nearly double that of the ungrafted gum (621.2 ± 1.1 cps), consistent with branched-network formation during grafting (Table 4). These enhanced swelling and viscosity properties are favourable for matrix-forming, sustained-release tablet applications. FTIR spectra of physical mixtures of sulfasalazine with ungrafted and grafted gum retained all principal drug peaks without shifting or disappearance, indicating no significant drug-polymer interaction over four weeks of storage.

Table 4. Swelling capacity and viscosity of ungrafted and grafted Eucalyptus obliqua gum

Parameter	Ungrafted Eucalyptus obliqua gum	Grafted Eucalyptus obliqua gum
Swelling capacity at 240 min (%)	389.5	716.0
Viscosity (cps, 32.7 °C)	621.2 ± 1.1	1188.6 ± 1.4

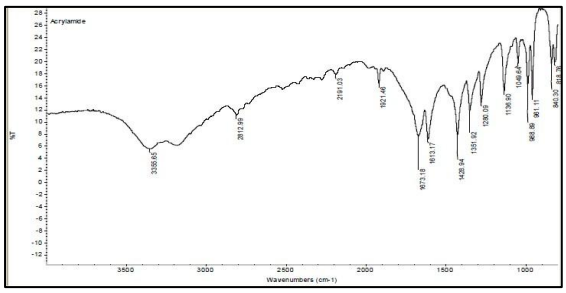

Figure 4. FTIR spectra of (a) Eucalyptus obliqua gum and (b) acrylamide

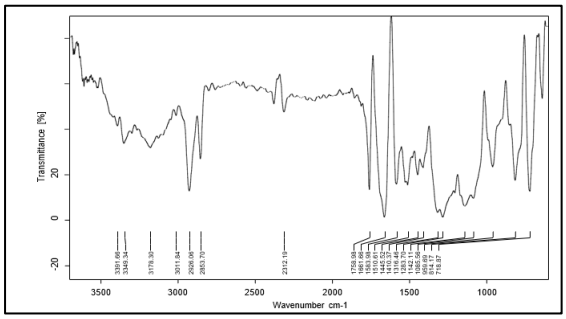

Figure 5. FTIR spectrum of acrylamide-grafted Eucalyptus obliqua gum

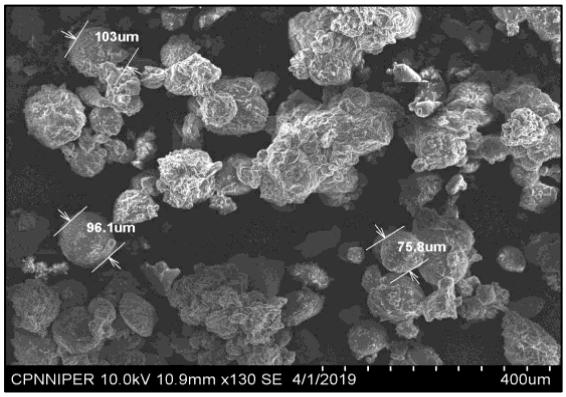

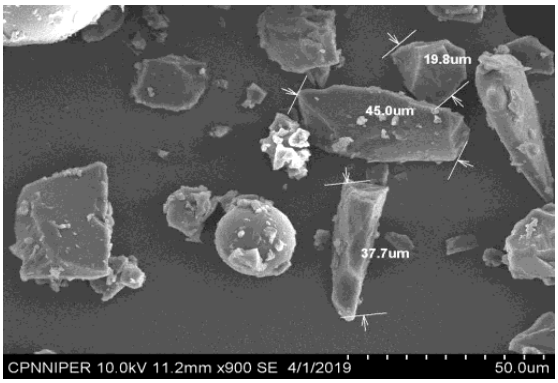

Figure 6. SEM images of (a) ungrafted and (b) grafted Eucalyptus obliqua gum

3.4 Precompression and post-compression evaluation of matrix tablets

Angle of repose (27.08-30.82° for UEO batches; 27.28-29.61° for GEO batches), Carr's index (8.48-12.21% for UEO; 8.48-11.60% for GEO) and Hausner's ratio (1.10-1.14 for UEO; 1.09-1.13 for GEO) were all within pharmacopoeial limits for good powder flow for all batches (Table 5). Post-compression parameters likewise met specification: thickness 3.23-3.50 mm, hardness 6.90-7.27 kg/cm², friability 0.24-0.49% (all < 1% limit), weight variation within ± 5% of the mean, and drug content 93.28-97.34% (Table 6), confirming uniform, mechanically robust tablets suitable for further dissolution testing.

Table 5. Precompression parameters of sulfasalazine tablet blends (UEO1-UEO5, GEO1-GEO5); n=3

Code	Angle of repose (°)	Bulk density (g/mL)	Tapped density (g/mL)	Carr's index (%)	Hausner's ratio
UEO1	30.823±0.808	0.435±0.006	0.482±0.016	9.677±0.809	1.107±0.022
UEO2	29.541±0.989	0.404±0.014	0.452±0.010	10.705±1.204	1.121±0.041
UEO3	29.417±0.627	0.425±0.007	0.484±0.021	12.209±1.113	1.142±0.069
UEO4	28.509±1.745	0.427±0.015	0.472±0.019	9.485±0.866	1.105±0.011
UEO5	27.084±0.981	0.380±0.005	0.419±0.003	9.278±0.628	1.102±0.008
GEO1	29.613±1.187	0.402±0.014	0.439±0.014	8.475±0.559	1.093±0.007
GEO2	28.807±0.906	0.383±0.010	0.425±0.012	9.784±0.412	1.109±0.017

Journal of Molecular Science
Journal of Molecular Science
Volume 36 Issue 2, Year of Publication 2026, Page 495-504
DoI-10.004687/1000-9035.2026.059

GEO3	29.326±1.419	0.439±0.004	0.484±0.008	9.257±1.154	1.102±0.026
GEO4	28.769±1.101	0.429±0.012	0.469±0.013	8.480±0.957	1.095±0.058
GEO5	27.281±1.546	0.386±0.008	0.437±0.013	11.596±1.364	1.131±0.017

Table 6. Post-compression parameters of sulfasalazine matrix tablets (UEO1-UEO5, GEO1-GEO5); n=3

Code	Thickness (mm)	Hardness (kg/cm²)	Friability (%)	Weight variation (mg)	Drug content (%)
UEO1	3.40±0.10	6.93±0.11	0.31	246.05±4.94	93.55±0.85
UEO2	3.43±0.11	7.17±0.29	0.26	249.90±4.92	93.28±0.85
UEO3	3.47±0.11	7.03±0.06	0.34	247.60±5.68	94.94±0.80
UEO4	3.30±0.20	7.00±0.36	0.32	249.35±6.13	95.86±0.85
UEO5	3.37±0.15	7.13±0.30	0.24	244.85±3.23	93.92±0.58
GEO1	3.40±0.17	6.93±0.15	0.42	250.70±5.29	96.60±0.57
GEO2	3.50±0.17	6.97±0.29	0.43	247.45±6.10	94.85±0.55
GEO3	3.37±0.11	6.90±0.26	0.49	252.75±5.60	96.69±0.89
GEO4	3.33±0.11	7.27±0.32	0.32	248.50±4.95	97.34±0.28
GEO5	3.23±0.11	7.07±0.32	0.45	246.60±4.60	95.59±0.89

3.5 In vitro drug release and mean dissolution time

Ungrafted-gum tablets (UEO1-UEO5) released 97-99% of the drug within 8-10 h, whereas grafted-gum tablets (GEO1-GEO5) sustained release for up to 18 h (Figure 4), with drug release decreasing progressively as the proportion of grafted gum increased (GEO1 > GEO2 > GEO3 > GEO4 > GEO5). This slower, more prolonged release from grafted-gum tablets is attributable to the higher swelling capacity and viscosity of the grafted gum, which forms a more coherent, slowly eroding gel layer around the tablet core, retarding water penetration and drug diffusion. Mean dissolution time (MDT) values confirmed this trend: MDT increased from 4.66-5.58 h for UEO1-UEO5 to 7.37-9.90 h for GEO1-GEO5 (Table 7), with GEO5 (the batch containing the highest grafted-gum-to-drug ratio, 1:0.75) showing the longest MDT (9.90 h) and was therefore selected as the optimized/best formulation among all ten Eucalyptus-based batches for further kinetic and stability evaluation.

Table 7. Mean dissolution time (MDT) of ungrafted and grafted Eucalyptus obliqua gum tablets

Code	MDT (h)	Code	MDT (h)
UEO1	4.66	GEO1	7.37
UEO2	4.81	GEO2	8.04
UEO3	5.15	GEO3	8.58
UEO4	5.24	GEO4	9.29
UEO5	5.58	GEO5	9.90

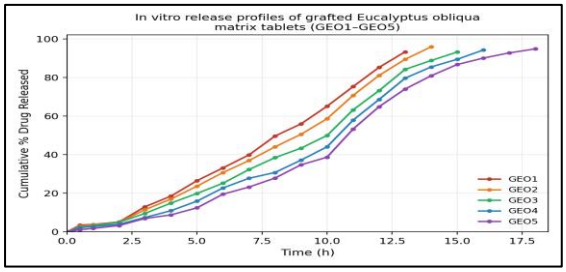

Figure 7. In vitro release profile of grafted Eucalyptus obliqua matrix tablets (GEO1-GEO5)

3.6 Release kinetics of optimized formulation (GEO5)

Release data of GEO5 were fitted to zero order, first order, Higuchi and Korsmeyer-Peppas models (Table 8, Figure 6). The Korsmeyer-Peppas model showed the best fit (R^2 = 0.9735), followed closely by the zero-order model (R^2 = 0.9658), while the first-order (R^2 = 0.8611) and Higuchi (R^2 = 0.8825) models fitted less well. The release exponent (n) of 1.366 (n > 1) indicates a super case-II transport mechanism, in which drug release is governed jointly by polymer chain relaxation/erosion and swelling rather than simple Fickian diffusion, and the overall release rate does not decline markedly over time — consistent with the good zero-order fit and the intended sustained-release performance of the grafted-gum matrix.

Table 8. Release kinetic model parameters for the optimized GEO5 tablet

Formulation	Zero order R^2	First order R^2	Higuchi R^2	Korsmeyer-Peppas R^2	n
GEO5	0.9658	0.8611	0.8825	0.9735	1.366

Journal of Molecular Science
Journal of Molecular Science
Volume 36 Issue 2, Year of Publication 2026, Page 495-504
DoI-10.004687/1000-9035.2026.059

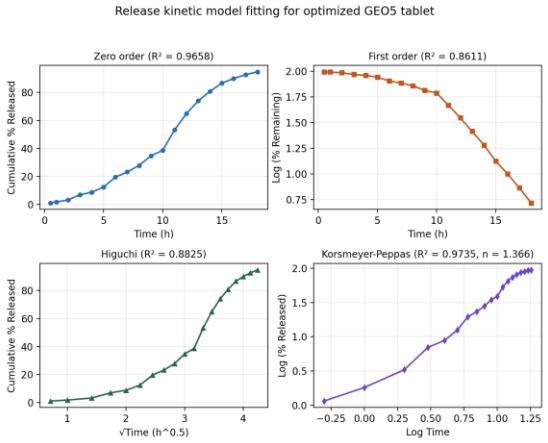

Figure 8. Release kinetic model fitting for the optimized GEO5 tablet

The optimized GEO5 formulation stored at 40°C ± 2°C / 75% ± 5% RH for three months showed no change in colour or odour at any interval. Hardness declined marginally (7.30 ± 0.26 to 7.13 ± 0.21 kg/cm²), drug content decreased slightly (95.22 ± 1.12% to 94.02 ± 0.55%) and friability increased marginally (0.44% to 0.54%), all remaining within acceptable pharmacopoeial limits (Table 9). Drug release profiles at 1, 2 and 3 months remained close to the initial (0-month) profile difference factor (f1) values of 2.73, 4.03 and 5.18, and similarity factor (f2) values of 87.23, 81.47 and 75.82 at months 1, 2 and 3 respectively, were within the accepted ranges (f1: 0-15, f2: 50-100), confirming that GEO5 was physically and chemically stable and released the drug consistently under accelerated storage conditions.

3.7 Accelerated stability of GEO5

Table 9. Stability data of optimized GEO5 tablets (40°C ± 2°C / 75% ± 5% RH)

Time interval	Hardness (kg/cm²)	Drug content (%)	Friability (%)	f1	f2
Initial (0 month)	7.30±0.26	95.22±1.12	0.44	-	-
1st month	7.23±0.21	94.94±0.97	0.44	2.73	87.23
2nd month	7.20±0.20	94.48±0.85	0.50	4.03	81.47
3rd month	7.13±0.21	94.02±0.55	0.54	5.18	75.82

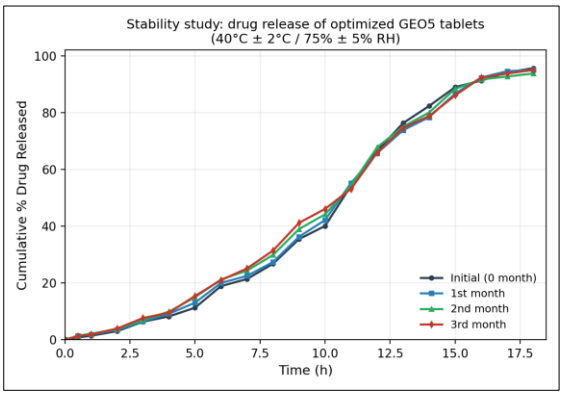

Figure 9. Drug release profile of GEO5 tablets during accelerated stability study

4. DISCUSSION

4.1 Novelty of acrylamide-grafted Eucalyptus obliqua gum as a carrier for sulfasalazine

Native Eucalyptus obliqua gum, like most unmodified plant exudate polysaccharides, hydrates rapidly and uncontrollably on contact with aqueous fluid, forms a loosely packed, easily eroded gel layer, and is prone to microbial spoilage and batch-to-batch variation in molecular weight. These properties make it unsuitable, on its own, for a matrix system that must retard drug release over many hours. In the present study, this limitation was addressed by covalently grafting acrylamide chains onto the gum backbone, which converts a weakly structured native polysaccharide into a reinforced semi-synthetic network. The novelty of the resulting carrier for sulfasalazine rests on three related points. First, to the best of the authors' knowledge, Eucalyptus obliqua gum has not previously been chemically modified and evaluated as a rate-controlling polymer for a poorly soluble, colon-relevant drug such as sulfasalazine; most literature on grafted gums as SR carriers has focused on more extensively studied gums (e.g., guar, xanthan, karaya), leaving Eucalyptus obliqua comparatively unexplored despite its local availability and low cost. Second, the modification itself is functionally novel in outcome rather than merely structural: grafting nearly doubled both the swelling capacity (389.5% → 716% at 240 min) and the apparent viscosity (621.2 → 1188.6 cps) of the gum (Table 4), and this combination directly translated into an extension of drug release from 8-10 h (ungrafted, UEO series) to up to 18 h (grafted, GEO series). A carrier is only "novel" in a meaningful pharmaceutical sense if the modification measurably changes performance, and here the same drug, tablet weight and compression process gave a more than two-fold increase in mean dissolution time (4.66-5.58 h to 7.37-9.90 h; Table 7) purely as a function of the polymer's grafted architecture. Third, the carrier was not developed empirically but through a statistically optimized, quality-by-design (Box-Behnken/RSM) route, so the grafted gum used in the tablets is a reproducible, model-verified material (predicted vs. experimental yield, grafting and grafting efficiency all within close agreement; Table 3) rather than a one-off laboratory product. Taken together — an under-explored natural gum, a functionally significant and reproducible modification, and demonstrated compatibility and stability with sulfasalazine — the grafted Eucalyptus

Journal of Molecular Science
Volume 36 Issue 2, Year of Publication 2026, Page 495-504
DoI-10.004687/1000-9035.2026.059

obliqua gum represents a genuinely new, low-cost, biodegradable alternative to conventional synthetic release-retardant polymers (e.g., HPMC, Carbopol, ethyl cellulose) for this drug.

4.2 Mechanism: how the grafting method and the resulting matrix system work

The synthesis mechanism proceeds through a ceric ion-initiated free-radical graft copolymerization. Ceric ammonium nitrate (CAN), a well-known redox initiator, forms a transient complex with the vicinal hydroxyl groups on the Eucalyptus obliqua gum backbone; collapse of this complex abstracts a hydrogen atom and generates a free-radical site on the polysaccharide chain while the cerium is reduced. This macroradical then acts as the initiation point for the vinyl monomer, acrylamide, which propagates outward as a covalently attached poly(acrylamide) side chain. Microwave irradiation was used in place of conventional thermal heating to drive this reaction: microwave energy couples directly with the polar hydroxyl/amide groups in the reaction mixture, producing rapid, volumetric (rather than surface-limited) heating. This shortens reaction time, improves uniformity of radical generation across the gum backbone, and reduces the extent of unwanted homopolymerization of free acrylamide, which is why the grafting efficiency of the optimized batch (48.94% experimental) was appreciably higher than that of poorly performing design points where monomer or initiator amounts were mismatched (as low as 3.08-9.62% grafting efficiency in batches with excess initiator or unfavourable monomer ratio; Table 2).

The relationship between the three process variables (monomer amount, initiator amount, temperature) and the three responses (% yield, % grafting, % grafting efficiency) was mapped using a Box-Behnken design, and this is why the process could be optimized rather than merely observed. The design fits a second-order (quadratic) polynomial to each response, capturing not only the direct effect of each factor but also two-factor interactions and curvature; the significant quadratic terms (A^2, B^2, C^2) in the yield model, for example, indicate that both monomer and initiator amounts have an optimum — too little produces insufficient radical sites/monomer for grafting, while too much promotes competing homopolymerization and radical termination, lowering the useful yield. The desirability-based numerical optimization then searched this modelled response surface for the single combination of factors (1.4 g acrylamide, 50 mg CAN, 60°C) that maximized all three responses simultaneously, and the close agreement between the model's predicted values and the experimentally verified checkpoint batch (Table 3) confirms that the underlying grafting chemistry, not chance, is what the model is describing.

Once formed into tablets, the grafted gum controls drug release through a combined swelling-erosion mechanism rather than simple diffusion. On contact with dissolution medium, water penetrates the tablet surface and hydrates the grafted polysaccharide-acrylamide network; because the grafted chains roughly double the material's water uptake capacity and viscosity relative to the ungrafted gum, they form a thicker, more cohesive and slower-eroding gel layer. This gel layer acts as a diffusional and physical barrier that the dissolved drug must cross, and as the outer gel layer becomes fully hydrated it erodes and exposes fresh polymer beneath — a moving boundary process that continues until the tablet is consumed. This is directly reflected in the release-kinetic analysis of the optimized GEO5 tablet: the Korsmeyer-Peppas release exponent of n = 1.366 (>1) is diagnostic of super case-II transport, in which polymer chain relaxation and erosion, not Fickian diffusion, are rate-limiting; the good zero-order fit (R^2 = 0.9658) is consistent with this, because erosion-controlled systems tend to release drug at a near-constant rate once the gel layer reaches a steady-state thickness. This is precisely why increasing the grafted-gum-to-drug ratio across GEO1 to GEO5 progressively slowed release and increased MDT (Table 7): more grafted polymer builds a thicker, longer-lived gel/erosion front around the drug core.

4.3 Justification of FTIR, DSC and SEM findings

FTIR was used as the primary chemical evidence that grafting had actually occurred, rather than the acrylamide and gum simply being physically mixed. Ungrafted Eucalyptus obliqua gum showed its own characteristic C-H, C=O and =C-H bands, while free acrylamide showed a sharp N-H stretch near 3355.65 cm^{-1} and a distinct C=O (amide I) band near 1647 cm^{-1}. In the grafted gum spectrum, these features did not simply appear as a superposition of the two starting materials; instead, the region around 2926 cm^{-1} broadened and merged, reflecting overlap of the gum's O-H stretch with the acrylamide N-H stretch on a shared, covalently linked backbone. A broadened, shifted composite band of this kind is the expected spectral signature of new covalent bonding/hydrogen-bonding environments created during grafting, and is therefore justified evidence that the monomer is chemically attached to the polysaccharide rather than merely co-present in a physical blend. FTIR of the sulfasalazine-gum physical mixtures further justified the choice of this carrier: all principal drug peaks (e.g., 1672.95 cm^{-1} C=O, 3299.41/3213.81 cm^{-1} N-H/O-H) persisted without shifting or disappearing after four weeks of contact, which is the standard spectroscopic criterion used to rule out significant drug-excipient interaction and to justify the compatibility of the

Journal of Molecular Science
Volume 36 Issue 2, Year of Publication 2026, Page 495-504
DoI-10.004687/1000-9035.2026.059

grafted gum with sulfasalazine for tablet formulation.

DSC was used to justify the grafting event from a thermal-behaviour standpoint, complementary to FTIR. Grafting restricts the mobility of the polysaccharide chains by tethering bulky poly(acrylamide) side chains to the backbone, which raises the energy required for chain segments to move past one another; this is why the grafted gum's thermal transition occurred at a higher temperature than that of the ungrafted gum or acrylamide alone. An upward shift in a thermal event is a well-accepted indirect indicator of increased cross-link/graft density and reduced free-volume/chain mobility, and it independently corroborates the FTIR evidence that a new, more thermally constrained macromolecular network had formed. DSC of sulfasalazine itself (melting endotherm at 160.14-164.78 °C, closely matching the 160-162 °C reference range; Table 1, Figure 1) was equally important as a purity/identity check, since a sharp, undepressed melting endotherm at the expected temperature confirms that the raw drug used throughout the study was authentic and of adequate purity before being incorporated into the grafted-gum matrix.

SEM provided the morphological justification that ties the FTIR/DSC chemical evidence to the functional (swelling, viscosity, release) data. The ungrafted gum surface was comparatively smooth, whereas the grafted gum showed a visibly rougher, more irregular and porous surface. This is the expected morphological consequence of grafting: poly(acrylamide) chains deposited and covalently anchored along the polysaccharide backbone disrupt what was originally a more uniform surface, creating additional surface area and micro-porosity. This SEM observation is not merely descriptive; it directly justifies the swelling and viscosity results, since a rougher, more porous surface offers more sites for water ingress and hydrogen bonding, which is mechanistically consistent with the near doubling of both swelling capacity and viscosity seen for the grafted gum relative to the ungrafted gum (Table 4). In this way, the three techniques form a coherent, mutually reinforcing line of evidence — FTIR confirms new chemical bonding, DSC confirms the resulting restriction in chain mobility, and SEM confirms the resulting change in surface architecture — that together justify why the grafted Eucalyptus obliqua gum behaves so differently from the native gum in both the swelling/viscosity data and the sustained drug-release performance reported in this study.

5. CONCLUSION:

Eucalyptus obliqua gum was successfully grafted with acrylamide by a microwave-assisted, ceric-ion-initiated method, and the process was efficiently optimized using a Box-Behnken design, giving an optimum condition of 1.4 g acrylamide and 50 mg ceric ammonium nitrate at 60°C. The grafted gum showed markedly higher swelling capacity and viscosity than the ungrafted gum, with FTIR, XRD and SEM confirming successful graft copolymer formation. When used as a matrix-forming polymer for sulfasalazine tablets, the grafted gum sustained drug release for up to 18 h (versus 8-10 h for the ungrafted gum), with the formulation GEO5 identified as optimal (MDT 9.90 h). Release from GEO5 followed a Korsmeyer-Peppas/super case-II transport mechanism and the formulation remained stable under accelerated storage for three months. These results support acrylamide-grafted Eucalyptus obliqua gum as a promising, low-cost, plant-based excipient for the development of sustained-release oral dosage forms of sulfasalazine and potentially other drugs requiring prolonged gastrointestinal release.

6. REFERENCES

1. Lee SH, Bajracharya R, Min JY, Han J, Park BJ, Han H. Strategic Approaches for Colon Targeted Drug Delivery: An Overview of Recent Advancements. Pharmaceutics [Internet]. 2020 Jan 15 [cited 2025 Nov];12(1):68–68. Available from: https://doi.org/10.3390/pharmaceutics12010068
2. Iswandana R, Putri KSS, Putri FA, Gunawan M, Larasati SA. Challenge and Development Strategy for Colonial drug delivery System. Pharmaceutical Sciences and Research [Internet]. 2022 May 18 [cited 2025 Oct];9(1). Available from: https://doi.org/10.7454/psr.v9i1.1251
3. Awad A, Madla CM, McCoubrey LE, Ferraro F, Gavins FKH, Buanz ABM, Gaisford S, Orlu M, Siepmann F, Siepmann J, Basit AW. Clinical translation of advanced colonic drug delivery technologies. Advanced Drug Delivery Reviews [Internet]. Elsevier BV; 2021 Dec 8 [cited 2025 Aug];181:114076–114076. Available from: https://doi.org/10.1016/j.addr.2021.114076
4. Roy D, Sarkar AN, Bachhar A, Das U, Mandal S. Gum Odina in focus: modification strategies, extensive characterization multifunctional applications, and comparative assessment with conventional gums. Journal of Biomaterials Science Polymer Edition [Internet]. 2025 Sept 12 [cited 2025 Dec];1–42. Available from: https://doi.org/10.1080/09205063.2025.2558696
5. Chandakavathe BN, Kulkarni RV, Mali A, Muthal A, Shinde V, Kulkarni R. Fabrication of sustainable modified fenugreek gum block copolymer in oral controlled drug delivery system: synthesis, toxicity, in vitro and in vivo pharmacokinetics. Research Square (Research Square) [Internet]. 2025 Mar 27 [cited 2025 Sept]; Available from: https://doi.org/10.21203/rs.3.rs-6231237/v1
6. Rabeh MI, Vora LK, Moore J, Bayan MF, McCoy CP, Wylie MP. Dual stimuli-responsive delivery system for self-regulated colon-targeted delivery of poorly water-soluble drugs. Biomaterials Advances [Internet]. 2023 Dec 21 [cited 2026 Jan]; 157:213735–213735. Available from: https://doi.org/10.1016/j.bioadv.2023.213735
7. Liaqat H, Badshah SF, Minhas MU, Barkat K, Khan SA, Hussain MD, Kazi M. pH-Sensitive Hydrogels Fabricated with Hyaluronic Acid as a Polymer for Site-Specific Delivery of Mesalamine. ACS Omega [Internet]. 2024 June 21 [cited 2025 Dec];9(26):28827–40. Available from: https://doi.org/10.1021/acsomega.4c03240
8. Jiang Y, Wang Y, Zhang Y, Zan X, Tong H, Tang S. Azo-

Journal of Molecular Science
Volume 36 Issue 2, Year of Publication 2026, Page 495-504
DoI-10.004687/1000-9035.2026.059

Linked 5-ASA Hydrogel Microparticles with Enzyme Shielding for Sustained Drug Release in Ulcerative Colitis Therapy. Biomacromolecules [Internet]. 2025 Oct 20 [cited 2025 Nov];26(11):7656–69. Available from: https://doi.org/10.1021/acs.biomac.5c01176

9. Khatibi N, Naimi-Jamal MR, Balalaie S, Shokoohmand A. Development and evaluation of a pH-sensitive, naturally crosslinked alginate-chitosan hydrogel for drug delivery applications. Frontiers in Biomaterials Science [Internet]. 2024 Nov 1 [cited 2025 Oct];3. Available from: https://doi.org/10.3389/fbiom.2024.1457540
10. Suhail M, Shao Y fang, Vu QL, Wu P. Designing of pH-Sensitive Hydrogels for Colon Targeted Drug Delivery; Characterization and In Vitro Evaluation. Gels [Internet]. 2022 Mar 3 [cited 2026 Mar];8(3):155–155. Available from: https://doi.org/10.3390/gels8030155
11. Bayan MF, Marji SM, Salem MS, Begum MY, Chidambaram K, Chandrasekaran B. Development of Polymeric-Based Formulation as Potential Smart Colonic Drug Delivery System. Polymers [Internet]. 2022 Sept 5 [cited 2025 Nov];14(17):3697–3697. Available from: https://doi.org/10.3390/polym14173697
12. Koev TT, Harris HC, Kiamehr S, Khimyak YZ, Warren FJ. Starch hydrogels as targeted colonic drug delivery vehicles. Carbohydrate Polymers [Internet]. 2022 Mar 26 [cited 2026 Jan]; 289:119413–119413. Available from: https://doi.org/10.1016/j.carbpol.2022.119413
13. Nanda N, Laware RB. Formulation Development and Optimization of Sulfasalazine SustainedRelease Matrix Tablets Using Grafted Natural Gums. International Journal of Drug Delivery Technology [Internet]. 2026 June 2 [cited 2026 June];16. Available from: https://doi.org/10.25258/ijddt.16.43s.69
14. Kumar M, SURAJPAL. MASTIC-G-POLY (ACRYLAMIDE): MICROWAVE-ASSISTED SYNTHESIS AND CHARACTERISATION. International Journal of Applied Pharmaceutics [Internet]. 2021 Mar 7 [cited 2025 Nov];228–34. Available from: https://doi.org/10.22159/ijap.2021v13i2.40551
15. Luan W, Sun L, Zeng Z, Xue W. Optimization of a polyvinyl butyral synthesis process based on response surface methodology and artificial neural network. RSC Advances [Internet]. 2023 Jan 1 [cited 2026 Jan];13(11):7682–93. Available from: https://doi.org/10.1039/d2ra08099k
16. Mazumder R, Mahanti B, Majumdar S, Pal R, Pahari N. Satranidazole-loaded chitosan/locust bean gum/xanthan gum polysaccharide composite multiunit pellets for colon targeting: in vitro–in vivo investigation. Beni-Suef University Journal of Basic and Applied Sciences [Internet]. 2022 Dec 21 [cited 2025 Nov];11(1). Available from: https://doi.org/10.1186/s43088-022-00333-w
17. Chandakavathe BN, Kulkarni R, Rajmane AD, Mane S, Waykule NJ. Development of Colon Targeted Extended Drug Delivery System for Mebendazole Using Grafted Natural Polymers. Indian Journal of Pharmaceutical Education and Research [Internet]. 2024 Aug 10 [cited 2025 Nov];58. Available from: https://doi.org/10.5530/ijper.58.3s.85